JOURNAL OF CATALYSIS 145, 683–696 (1994)

Modeling of Pulsed Gas Transport Effects in the TAP Reactor System

Bai Sheng Zou,* Milorad P. Dudukovic,* and Patrick L. Mills†

*Chemical Reaction Engineering Laboratory, Washington University, One Brookings Drive, St. Louis, Missouri 63130-4899; and †Corporate Catalysis Center, DuPont Company, Experimental Station, Wilmington, Delaware 19880-0262

Received May 20, 1993; revised March 29, 1994

A method for quantification of the gas pulse transport in the TAP (temporal analysis of products) reactor system is presented. Particular components of the TAP reactor system that are considered include the high-speed pulse valve, the packed-bed microreactor, and the high vacuum system. The model developed for the pulse valve allows an *a priori* evaluation of the inlet pulse intensity as a function of feed gas conditions and valve settings. Two independent models that account for simultaneous diffusion, adsorption, and desorption are developed for the packed-bed microreactor. The first model describes the transient response of the microreactor packed with nonporous particles and is primarily intended for assessment of gas pulse transport in the interparticle region and on the particle surface. The second model is similar, except that it accounts for diffusion of the gas pulse in porous particles. Molecular beam transport and an evaluation of backscattering in the vacuum system behind the microreactor are also quantified. Evaluation of model parameters by a time-domain parameter estimation technique is also described and illustrated through several applications including estimation of diffusivities and desorption parameters. The modeling approach presented here forms a basis for further quantification of TAP studies.

INTRODUCTION

The TAP (temporal analysis of products) reactor system was introduced about 6 years ago as an experimental technique for studying kinetics and mechanisms of gas-phase heterogeneous catalyzed reactions (1, 2). The working concept is based upon measurement of the transient responses of various gas-phase reaction products obtained from a packed-bed microreactor as a result of pulsing reactants from high-speed molecular-beam type valves. The input pulse can be introduced using a variety of pulse formats so that the dynamics of the gas–solid transport–kinetics interactions can be studied. Typical examples of input pulse formats include single-valve pulsed experiments with signal averaging, single-valve multipulse experiments, and dual-valve pump–probe experiments. Additional details on the experimental capabilities of the TAP reactor system are given in the above-cited references.

The mode of gas transport that occurs in the TAP reactor system differs from that in conventional transient response catalytic reactors. As shown in Fig. 1, the input pulse in a TAP microreactor, whose composition can be a binary or multicomponent mixture of reaction gases, is introduced from one or both of the molecular beam valves, whose total pressures are near atmospheric. No carrier gas, such as helium or nitrogen, is used. Instead, the exit of the microreactor is open so that it is exposed to the pumping of a high vacuum chamber whose background pressure is between 10^{-7} and 10^{-8} Torr (1 Torr = 133.3 N m^{-2}). Therefore, the total pressure of the gas pulse varies between these two extreme limits over the entire microreactor length. In contrast, conventional pulse reactors typically operate at a total pressure of about 1 atm, and the amount of reactant introduced is small enough that it has a negligible effect on the instantaneous total pressure. At sufficiently low input pulse concentrations, the above method of introducing reactants into the TAP microreactor will result in a significant reduction in the local pressure in the microreactor inlet section, so that gas transport in the catalyst zone is dominated by Knudsen diffusion. Once the gas pulse exits the microreactor, the local pressure is low enough that gas transport is described by free molecular flow (3). The ability to perform transient response experiments in the limit of Knudsen diffusion minimizes collisions between gas-phase molecules so that the transient responses of product molecules in the TAP

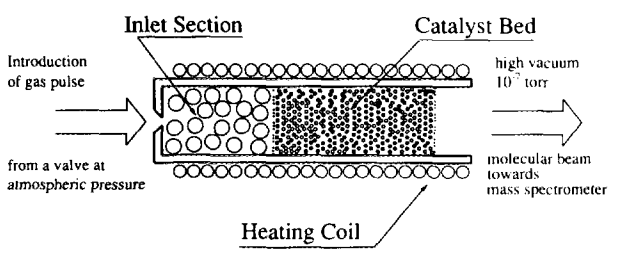

FIG. 1. The TAP microreactor.

0021-9517/94 $6.00

microreactor should be indicative of gas–solid transport–kinetics interactions. This may allow detection of short-lived unstable reaction intermediates which otherwise could not be measured using transient techniques, where the frequency of gas–gas collisions is much greater (4).

For example, TAP reactor experiments for the selective oxidation of *n*-butane over vanadyl pyrophosphate at 420°C using a 4 : 1 oxygen : butane mixture show that butene, butadiene, and furan can be detected as desorbing reaction intermediates in the reaction pathways to maleic anhydride (1). Conventional pulsed reactor experiments by Pepera *et al.* (5) at atmospheric pressure for the same catalytic system did not result in the detection of these same intermediates in the gas phase. Experiments by Centi *et al.* (6) and Morselli *et al.* (7) using a fixed-bed microreactor in the classical steady-flow mode under atmospheric pressure verify the existence of these three intermediates, but the feed gas was hydrocarbon-rich, indicative of highly reducing conditions. These results suggest that the TAP reactor, when operated in the pulsed high vacuum mode illustrated in Fig. 1, provides a means of reducing gas phase collisions where reaction intermediates can be detected.

Inspection of Fig. 1 suggests that the inlet section of the TAP microreactor could be packed in different ways to ensure that the pulsed gas is at the limit of Knudsen diffusion before reaching the catalyst bed. The method illustrated in Fig. 1 uses packing in the inlet section that is inert under reaction conditions, while the catalyst bed is located downstream (1). Gas-phase pyrolysis experiments by Svoboda *et al.* (8) involving model organometallic precursors used inert quartz granules as well as inert boron nitride packing throughout the entire microreactor length. Knudsen diffusion was obtained by reducing the pulse valve pressure until the normalized transient responses were invariant, which is indicative of linearity. Zou (9) used an empty inlet zone so that expansion of the pulsed gas resulted in the limit of Knudsen diffusion being attained at the inlet to the catalytic bed. The net effects of using these different methods to pack the inlet section are to alter the characteristic entry length required for the gas to achieve the desired Knudsen diffusion limit and to either increase or decrease the time resolution of the resulting transient response.

Although qualitative insight into the heterogeneous catalysis mechanism can be obtained by examination of the TAP transient response, quantitative values for kinetics and equilibrium parameters of elementary reaction steps require detailed mathematical models that account for the transient processes that occur during the passage of a gas pulse through the microreactor. In principle, these models should allow discrimination between various assumed or postulated reaction mechanisms through parameter estimation techniques (8, 10). Before detailed models are developed, however, a basic understanding of the transport processes that occur during the passage of a pulse in the absence of reaction must be established. Presumably, the parameters in these models can be determined through independent experiments involving reactant or product molecules under the same conditions as those under which the reactions are performed. Once these are established, parameters in various reaction mechanisms can be determined by time-domain parameter estimation techniques similar in concept to those used to analyze reaction engineering tracer-type experiments (11). Rigas *et al.* (12) described an example of this approach by which adsorption rate and kinetic constants for the incorporation of oxygen into silver metal catalysts for ethylene epoxidation were determined. However, this effort is in an early stage of development and has not been used on other types of reacting systems.

In their initial paper on the TAP reactor system, Gleaves *et al.* (1) described a basic transport–kinetic-type model to describe the transient response for the TAP reactor under conditions where the gas transport could be described by Knudsen diffusion. The effect of using various approaches to pack the microreactor on the transient response was not discussed. In addition, the mathematical basis for using the suggested boundary conditions for the governing model equations was not given. It is well known in the reaction engineering literature on tracer techniques (13) that the specification of boundary conditions can have a significant effect on the model-predicted transient responses under certain conditions. Also, as shown by Zou (9), different techniques for packing the TAP microreactor require the use of specific forms for the model equations used to describe the pulse transport and associated boundary conditions. Finally, the transient responses measured in TAP experiments actually represent the combined response of the pulse valve, kinetic–transport interactions in the packed-bed microreactor, pulse transport through the vacuum system, and the response dynamics of the mass spectrometer detector. Hence, an assessment of the contribution of the various system components to the overall measured response needs additional clarification.

The primary objective of this paper is to set forth fundamental models that describe the pulse transport in a TAP system for situations where the microreactor contains either nonporous or porous packing. The emphasis here is placed on a model that accounts for interparticle pulsed gas transport by Knudsen diffusion with linear and reversible adsorption in the case of nonporous particles. For porous particles, intraparticle transport in the catalyst pores by Knudsen diffusion is also included along with the above-mentioned transport effects. In addition to developing models for the packed-bed microreactor, a phe-

nomenological model for evaluating the pulse intensity from the molecular beam is also described. Finally, models are given for transport of the gas pulse from the microreactor exit to the mass spectrometer that account for the relationship between species flux and concentration, as well as possible backscattering effects. Applications of the models to describe the effect of the pulsed gas molecular weight, the effect of the length of the packed-bed zone, and the extraction of heats of adsorption from transient data are also given.

EXPERIMENTAL

A simplified diagram of the TAP reactor system used in this study is given in Fig. 2. This particular design was a precursor to the current commercial version and consisted of three vacuum chambers. These chambers house the pulse valve manifold, the microreactor, and the quadruple mass spectrometer detector. Vacuum is generated by two oil diffusion pumps for the microreactor and differentially pumped detector chamber and by an ion pump at the end of the anaytical chamber. Average pressures on the order of 10^{-7}, 10^{-8}, and 10^{-9} Torr can be maintained in the three chambers, respectively.

The reactor chamber is shaped like a cube whose edge dimension is 2 ft. It contains the catalytic microreactor, the molecular beam valve, and various power and reactant feed ports and lines. The interior of the reactor chamber can be accessed through circular ports located on each face. The bottom of the reactor chamber is connected to a 10-in. diffusion pump which can generate a background vacuum of about 10^{-7} Torr. The reactor chamber is separated from the differential chamber by a shutter valve that allows the transport of gas molecules from the reactor chamber into the differential chamber and the analytical chambers.

The differential chamber is used for removal of excess gas molecules so that only a small fraction of the reactant and product molecules that exit the reactor chamber can reach the analytical chamber. This chamber is a four-way cross that is welded together with pipes whose diameters are 7 and 5.5 in., respectively. One pipe contains a cold trap and another connects to a 6-in. diffusion pump. The diffusion pump under the differential chamber generates a vacuum on the order of 10^{-8} Torr.

The analytical chamber houses the quadruple mass spectrometer detector head. A Varian 8-in. ion pump with a rated pumping speed of about 400 liters/second is located at the end of the analytical chamber; it maintains a background vacuum on the order of 10^{-9} Torr. This chamber contains a 5.5-in. six-way cross and a 5.5-in. two-way nipple and has an overall length of about 20 in. One of the side flanges of the cross contains the mass spectrometer head, while the remaining flanges are connected to the ion pump and the intermediate chamber. In the newer version of the TAP system, the ion pump has been replaced by a turbomolecular pump. Also, the volume and shape of the vacuum chambers have been altered so that the distance between the mass spectrometer head and the microreactor exit has been reduced. The need for these changes is supported by the results of this study.

The key components of the TAP system are enclosed in the above-mentioned high vacuum chambers. Additional details are given in the review by Gleaves *et al.* (1).

The experiments described in a later section used nonporous glass beads as a microreactor packing and gases having various molecular weights to test the models. The beads and gases were obtained from commercial sources and used without additional treatment.

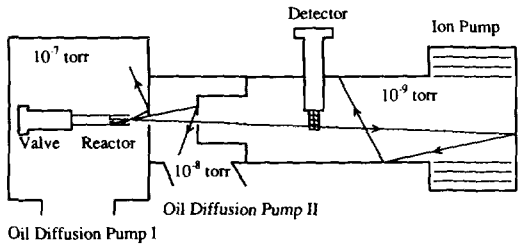

FIG. 2. Simplified schematic of the TAP system.

MATHEMATICAL MODELS

Model for the Pulsing Valve

An analysis of the fast pulsing valve by Zou (9), based on a phenomenological model, yields an equation for calculating the total number of molecules per pulse, N_t, that are introduced into the microreactor. The final result of this analysis is the following expression:

$$N_t = \beta \sqrt{\frac{\gamma}{RM}} \frac{P_0}{\sqrt{T_0}} \left(\frac{\gamma+1}{2}\right)^{-(\gamma+1)/2(\gamma-1)} \left[\frac{1}{2.45}(I_t - I_{t0})^2 + (I_t - I_{t0})(D_t - I_t)\right]. \quad [1]$$

The parameters that appear in Eq. [1] are defined in the Appendix. Inspection of Eq. [1] shows that the total number of molecules introduced per pulse is proportional to the valve pressure P_0. This, per se, is intuitively obvious, but the model also provides a quantification of the pulse in terms of valve settings. D_t in Eq. [1] is the duration time, which is controlled by the duration setting D of the valve drive. The variable I_t is the opening time, which is controlled by the intensity setting I of the valve drive. D_t and I_t were empirically related to the valve settings D and I, respectively, for our Newport BV-100 valve by the

following empirical equations:

$$D_t = 67.02 + 13.75D - 0.1D^2 + 0.000385D^3 \quad [2]$$

$$I_t = 8.5I + 140. \quad [3]$$

By setting the parameters I and D, and knowing the valve pressure P_0 and temperature T_0, the number of molecules introduced per pulse can now be predicted. Equation [1] can predict the experimental results for N_t with relative errors of less than 4.4% when the valve settings are $15 < I \leq 30$ and $15 < D \leq 60$, which covers the range for the transient experiments described here.

Model for the Microreactor

Model for a catalyst bed of nonporous particles. In the following development, the rate constants used are per unit catalyst weight. Although other bases can be selected, this choice is convenient since the results will be independent of particle density and bed porosity.

The model equations given below assume that a gas phase species A undergoes linear and reversible adsorption according to

$$A(g) \underset{k_2}{\overset{k_1}{\rightleftharpoons}} A(ads), \quad [4]$$

where k_1 and k_2 are the adsorption and desorption rate constants, respectively. A single adsorption process is used to illustrate the mathematical principle without messy algebra. This model can handle more complex kinetic rate forms such as $r = k_1C_1 + k_2C_2 + \cdots$, and even a network of reactions and adsorptions, as long as there is no nonlinear rate. Linear and reversible adsorption are used, since the number of gas–gas collisions is negligible compared to the number of gas–solid collisions under a pressure of 10^{-7} Torr and low surface coverage is obtained for single pulse experiments. A typical reactor loading of 2 g of nonporous particles would have a total surface area of 0.1 m^2/g. A single pulse of 10^{15} molecules/pulse would generate 0.0001 monolayers, assuming total adsorption. As a result, the amount of adsorption during a data collection sequence involving 100–200 pulses would amount to 1–2% of the total surface area. When porous particles are used, the surface coverage will be even lower due to their large surface area.

The governing mass balance equations are:

(a) mass balance for species A in the gas phase,

$$\varepsilon \frac{\partial C}{\partial t} = D_L \frac{\partial^2 C}{\partial x^2} - \rho_p(1 - \varepsilon)(k_1C - k_2C_{ads}), \quad [5]$$

where D_L is the effective Knudsen diffusion coefficient for species A in the randomly packed bed;

(b) mass balance for adsorbed species A on the solid phase,

$$\frac{\partial C_{ads}}{\partial t} = k_1C - k_2C_{ads}; \quad [6]$$

(c) mass balance for species A in the gas phase in the packed inlet section,

$$h_0^* \frac{\partial C^*}{\partial t} = D_L \left.\frac{\partial C}{\partial x}\right|_{x \to 0}. \quad [7]$$

The parameter h_0^* in Eq. [7] is the equivalent length of an empty inlet tube that has the same void space as an inlet section which is packed with inert packing. When the diameter of the inert packing in front of the catalyst bed is much larger than the mean diameter of the catalyst particles, the flow resistance in the catalyst bed will be much larger than the flow resistance in the glass beads section. In this case, the gas in the inert section approaches perfect backmixing. The justification for this assumption is discussed by Zou (9).

The boundary conditions for species A in the gas phase are

$$\text{at } x = 0, \quad C = C^*, \quad [8]$$

and

$$\text{at } x = h, \quad C = 0. \quad [9]$$

The experimental conditions are controlled so that the transport of molecules in the catalyst bed is by Knudsen diffusion and the flow at the exit of the microreactor is in the free molecular flow regime. The boundary condition at the microreactor exit given by Eq. [9] is the approximation obtained by equating the diffusion flux at the bed exit to molecular flow of gas (vC) when the mean gas velocity (v) is very large (6). If one assumes that molecules have the same temperature as the catalyst bed, the mean velocity (v) of the molecules can be calculated by using the kinetic theory of gases (14): $v = \sqrt{8RT/\pi M}$. If continuity of flux and concentration at the exit boundary is assumed, then the rigorous boundary condition is

$$\text{at } x = h, \quad -D_L \partial C/\partial x\,|_{h^-} = vC\,|_{h^-} \quad [10a]$$

$$C\,|_{h^-} = C\,|_{h^-}. \quad [10b]$$

Equations (10a) and (10b) can be cast into dimensionless form and rewritten as

$$\text{at } \eta = 1, \quad C\,|_{1^+} = -\varepsilon_1 \partial C/\partial \eta\,|_{1^-} \quad [11a]$$

$$C\,|_{1^-} = C\,|_{1^-}, \quad [11b]$$

where $\eta = x/h$ and $\varepsilon_1 = D_L/(vh)$. For oxygen at room temperature, the mean gas velocity $v = 44{,}500$ cm/s, so that v is typically a very large number. For oxygen flowing through a bed of 0.210-mm glass beads, the Knudsen diffusion coefficient is $D_L = 23$ cm^2/s. If the bed length is 3 cm, then $\varepsilon_1 = D_L/(vh) = 1.723 \times 10^{-4}$. Since ε_1 is such a small number, and the gradient $\partial C/\partial\eta$ cannot be large, Eqs. [11a] and [11b] reduce to Eq. [9].

The magnitude of the velocity of the oxygen would suggest that supersonic flow exists and that a shock wave would occur at an upstream location where the sonic velocity is achieved. However, these phenomena are associated with flow in the continuum regime and cannot occur in the randomly packed bed and low pressure conditions that exist in the catalytic zone of the TAP microreactor.

The initial conditions correspond to specified concentrations for the pulsed gas in the interparticle region and on the catalyst surface,

$$\text{at } t = 0, \quad C = C_{ads} = 0, \qquad [12]$$

and

$$\text{at } t = 0, \quad C^* = C_0^*. \qquad [13]$$

Here, $C^* = C_0^*$ implies that the gas component A is pulsed into the microreactor inlet section with an initial concentration of C_0^*, where the latter quantity is obtained by dividing N_t from Eq. [1] by the void volume of the inlet section.

Solution of Eqs. [5]–[13] eventually yields the expression

$$\bar{C}(s, x) = \frac{h_0^* C_0^* \sinh \phi(h - x)}{h_0^* s \sinh \phi h + D_L \phi \cosh \phi h} \qquad [14]$$

for the Laplace-transformed concentration of species A in the gas phase, here ϕ is defined by

$$\phi = \sqrt{\rho_p(1 - \varepsilon)\frac{k_1 s}{D_L(k_2 + s)} + \frac{s\varepsilon}{D_L}}. \qquad [15]$$

The Laplace transform of the molar flux of species A at the microreactor exit $x = h$ is

$$\bar{N}(s) = -D_L \left.\frac{\partial \bar{C}}{\partial x}\right|_{x=h} = \frac{D_L h_0^* C_0^* \phi}{h_0^* s \sinh \phi h + D_L \phi \cosh \phi h}. \qquad [16]$$

The moments of the TAP response curve can now be related to the key model parameters, namely, the effective Knudsen diffusivity D_L, the adsorption equilibrium constant $K = k_1/k_2$, and the microreactor bed length h. The expressions for the moments can be obtained from the above expression for the Laplace transform of the molar flux $\bar{N}(s)$. The details are omitted for brevity, so only the final results are given. The final expression for the first absolute moment or mean of the TAP response curve is

$$\bar{t} = \frac{\int_0^\infty tN(t)\,dt}{\int_0^\infty N(t)\,dt} = -\left.\frac{d\bar{N}(s)/ds}{\bar{N}(s)}\right|_{s=0} = \frac{h^2\varepsilon}{2D_L}\left(1 + 2\frac{h_0^*}{h\varepsilon} + \rho_p\frac{(1 - \varepsilon)}{\varepsilon}\frac{k_1}{k_2}\right), \qquad [17]$$

where k_1/k_2 can also be interpreted as K. Similarly, the final expression for the second central moment or variance is

$$\sigma^2 = \overline{(t - \bar{t})^2} = \frac{\int_0^\infty t^2 N(t)\,dt}{\int_0^\infty N(t)\,dt} - (\bar{t})^2 = \left(\frac{h^2\varepsilon}{D_L}\right)^2\left(\left(\frac{D_L\rho_p(1 - \varepsilon)k_1}{2(h\varepsilon)^2 k_2^2}\right) + \frac{1}{6}\left(1 + 2\frac{h_0^*}{h\varepsilon} + \rho_p\frac{(1 - \varepsilon)}{\varepsilon}\frac{k_1}{k_2}\right)^2 + \frac{1}{3}\left(\frac{h_0^*}{h\varepsilon}\right)^2\right). \qquad [18]$$

Equations [17] and [18] contain the equivalent length h_0^* of the inlet section, and represent the generalization of the moments equations presented by Gleaves *et al.* (1). When h_0^* tends to zero, and $h_0^* C_0^*$ is kept constant, Eq. [16] is reduced to the expression developed by Gleaves *et al.* (1), except that the terms containing the adsorption rate constants k_1 and k_2 have a different form since different units were used. The above equations show that the first absolute moment of the TAP response curve for a linearly adsorbing species depends on the effective Knudsen diffusion coefficient D_L and the adsorption equilibrium constant K. The variance has the same dependence, except that it is more complex in form and contains the expression for the first absolute moment as part of its functional dependence.

Model for a catalyst bed of porous particles. Many catalysts are porous due to their methods of preparation. To describe gas transport of a single gas component in the Knudsen diffusion regime for a TAP microreactor

packed with porous particles, two diffusivities are needed. The first is used to describe Knudsen diffusion through the catalyst bed, while the second describes the diffusion in the catalyst particles. This is a reasonable approach if the pore-size distribution in the catalyst particles is unimodal and narrow. The mathematical model must now account for the following transport steps: (a) Knudsen diffusion of a gas component through the catalyst bed, (b) Knudsen diffusion of the gas component in the catalyst particles, and (c) linear adsorption and desorption of the gas component on the inner surface of the catalyst particles. The model developed below is similar to the model for a conventional pulsed fixed bed reactor (15), except that there is no convective flow term. The time-dependent flux for species A at the microreactor exit can be obtained by solving the following system of material balance equations:

(a) mass balance for species A in the gas phase of the interparticle void region,

$$\varepsilon \frac{\partial C}{\partial t} = D_L \frac{\partial^2 C}{\partial x^2} - \frac{3D_S(1-\varepsilon)}{R}\left(\frac{\partial C_p}{\partial r}\right)\Bigg|_{r=R}; \qquad [19]$$

(b) mass balance for species A in the intraparticle voids of the particles,

$$\beta \frac{\partial C_p}{\partial t} + \rho_p \frac{\partial C_{ads}}{\partial t} = D_S\left(\frac{\partial^2 C_p}{\partial r^2} + \frac{2}{r}\frac{\partial C_p}{\partial r}\right); \qquad [20]$$

(c) linear, reversible adsorption for species A,

$$\frac{\partial C_{ads}}{\partial t} = k_{ads}(C_p - C_{ads}/K_a). \qquad [21]$$

The boundary conditions for the particles are specified concentration of species A at the surface and symmetry:

$$\text{at } r = R, \quad C_p = C; \qquad [22a]$$

$$\lim_{r\to 0}\left\{r^2 \frac{\partial C_p}{\partial r}\right\} = 0. \qquad [22b]$$

The boundary conditions for the catalyst bed are the same as Eqs. [7], [8], and [9] for the bed of nonporous catalyst particles, while the initial conditions are similar to Eqs. [12] and [13]:

$$\text{at } t = 0, \quad C = C_p = C_{ads} = 0, \qquad [23a]$$

and

$$\text{at } t = 0, \quad C^* = C_0^*. \qquad [23b]$$

The solution of Eqs. [19]–[23] eventually yields the following equation for Laplace-transformed concentration of species A in the gas phase:

$$\bar{C}(s,x) = \frac{h_0^* C_0^* \sinh \Psi(h-x)}{D_L \Psi \cosh h\Psi + h_0^* s \sinh h\Psi}. \qquad [24]$$

The Laplace transform of the molar flux at the microreactor exit is

$$\bar{N}(s) = -D_L \frac{\partial \bar{C}}{\partial x}\Bigg|_{x=h} = \frac{D_L h_0^* C_0^* \Psi}{D_L \Psi \cosh h\Psi + h_0^* s \sinh h\Psi}. \qquad [25]$$

The parameters Ψ and ψ are defined by

$$\Psi^2 = \frac{s\varepsilon}{D_L} + \frac{3D_S(1-\varepsilon)}{R^2 D_L}(R\psi \coth R\psi - 1) \qquad [26]$$

and

$$\psi^2 = \frac{\beta s}{D_S} + \frac{\rho_p k_{ads} s}{D_S(s + k_{ads}/K_a)}. \qquad [27]$$

As in the previous case for the nonporous particles, the moments of the TAP response curve can be related to the various model parameters. The final expression for the first absolute moment or mean is

$$\bar{t} = \frac{h^2\varepsilon}{2D_L}\left(1 + 2\frac{h_0^*}{h\varepsilon} + \frac{1-\varepsilon}{\varepsilon}(\beta + \rho_p K_a)\right). \qquad [28]$$

Comparing Eq. [17] to Eq. [28], it can be seen that the difference between $\bar{t}$ for the bed of porous particles and $\bar{t}$ for the bed of nonporous particles is that there is an extra particle porosity term β in Eq. [28].

The variance does not exist for this model for porous particles because the integration of $\int_0^\infty t^2 N(t)\,dt$ does not converge. Physically, this is caused by the fact that the particles can release the gas molecules that originally diffused into them at extremely large time. Mathematically, it also implies that the integration $\int_0^\infty t^2 N(t)\,dt$ tends to infinity since $N(t)$ decays slower than t^{-3}.

Time-Domain Solution of the Model Equations

Time-domain values for the flux at the microreactor exit can be obtained by numerical inversion of the Laplace

transforms (9) using Eqs. [16] and [25]. This procedure for obtaining the time-domain solution is more efficient than using numerical integration to solve the original governing differential equations.

The fast Fourier transform (FFT) method is used in this work for numerical inversion of the Laplace transform. This method involves replacing the Laplace transform variable s by a complex variable $s = c + 2\pi if$, where c and f are real, so that the Laplace transform is converted to a Fourier transform in the complex domain. The resulting expressions are then inverted to obtain the time-domain solution by the FFT method (16).

An illustration of time-domain flux at the microreactor exit using the model for nonporous particles with assumed values for the model parameters is shown in Fig. 3. The particular model parameters are given on the figure caption and correspond to a finite rate of adsorption. The time-domain flux at the microreactor exit for the case of no adsorption ($k_1 = k_2 = 0$, dashed line) is also shown for comparison purposes. For both curves, $h_0^* C_0^* = 1$ (mol/cm^2), which means that a unit impulse of gas is injected into the microreactor. Clearly, adsorption increases the mean of the curve and its spread around the mean, which are also indicated by the expressions for the mean and variance derived from the method of moments, Eqs. [17] and [18].

Figure 4 compares two different model-predicted responses using the same values for bed Knudsen diffusivity, bed length, and bed porosity, where one of the responses corresponds to the model for porous particles (dashed line) while the other applies to the model for nonporous particles (solid line). For the assumed model parameters, intraparticle diffusion affects the shape of the curve sufficiently that it would have to be included if the simulations were indicative of experimental data obtained from an actual porous catalyst.

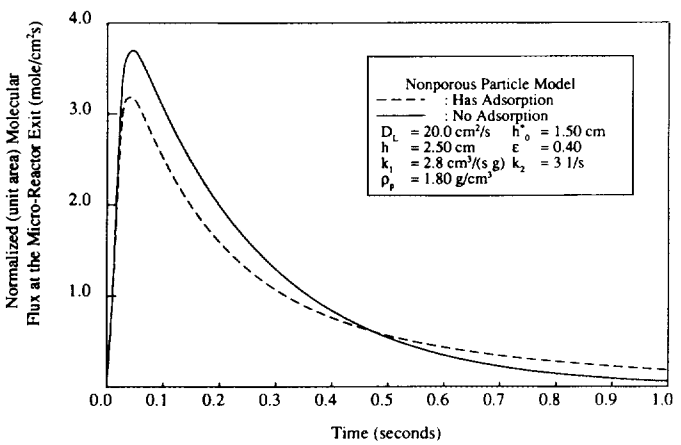

FIG. 3. Fluxes at the exit of the microreactor packed with nonporous particles.

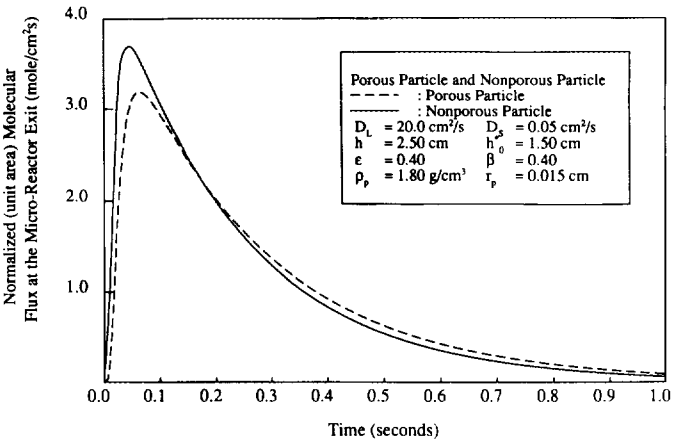

FIG. 4. Comparison between the porous and the nonporous particle models.

Model for Free Molecular Flow Downstream of the Microreactor Exit

A key issue that arises during interpretation of the measured TAP responses is concerned with how the number density of molecules in the mass spectrometer detection zone is related to the flux or the concentration at the microreactor exit. It will be shown that the data can be properly interpreted if the following two modes of gas transport from the microreactor exit to the mass spectrometer detection chamber are considered: (1) the gas molecules are transported directly from the microreactor exit to the detector by molecular beam flow or (2) the gas molecules are transported by repeated collisions with the walls of the enclosure via backscattering flow. The molecules which pass the ionization zone of the mass spectrometer either come directly from the microreactor or come indirectly from the microreactor after collisions with the vacuum chamber walls. Those which come directly are classified as molecular beam flow; those which collide with the walls and are measured by mass spectrometer again are classified as backscattering flow.

Molecular beam flow. In molecular beam flow as applied to the TAP microreactor, it is assumed that all the gas molecules travel in a straight parallel line toward the mass spectrometer detector, and that those which pass through the ionization zone of the mass spectrometer are not reflected back. The justification for the assumption of a straight line-of-flight is provided by the fact that when molecules exist in the free molecular flow regime, the number of gas–gas collisions between the molecules is negligible (3). Hence, a molecule will travel in a straight line unless it hits a wall. When the microreactor exit is directed toward the ionization cage of the mass spectrometer, the molecules that exit the microreactor should travel in a straight path and intersect the mass spectrometer measurement volume. This assumption was confirmed

by a Monte Carlo simulation (9). Molecules that pass through the ionization cage without ionization are not reflected back to any measurable degree, since the measured transient responses do not contain multiple peaks indicative of molecular beam backscattering.

It is also important to note that the response curve measured by the mass spectrometer does not correspond exactly to the flux versus time curve at the exit of the microreactor because of distortion introduced by the gas pulse transport between the exit of the microreactor and the mass spectrometer detector. Since the assumption that molecules move in parallel lines with Maxwellian velocity distribution agrees with Monte Carlo calculations (9), the flux curve at the microreactor exit can be related to the response curve measured by the mass spectrometer using the following analysis.

Let the distance between the microreactor exit and the detector be L_m, and let the effective length of the detector zone be d_m. The detector zone would correspond to the ionization cage of the mass spectrometer. The molecules that exit the microreactor at the same time will pass through the detector zone at different times due to the Maxwellian velocity distribution.

Suppose that at time t_i, the total flux at the exit of the microreactor is $AN(t_i)$, where A is the cross-sectional area of the microreactor. The total number of molecules that exit the microreactor at time t_i during time interval dt_i is $AN(t_i)\,dt_i$. At a later time t, of all the molecules that exit the microreactor at time t_i, only those among them which have a velocity between $L_m/(t - t_i)$ and $(L_m + d_m)/(t - t_i)$ will be in the M.S. detector zone. Let $f(U)$ be the velocity distribution density function. The number of molecules that have left the microreactor exit in the interval dt_i at t_i and traveled the distance between L_m and $L_m + d_m$ by time t is given by

$$AN(t_i)\,dt_i \int_{L_m/(t-t_i)}^{(L_m+d_m)/(t-t_i)} f(U)\,dU. \qquad [29]$$

For every t_i such that $0 < t_i < t$, some molecules have exited the microreactor at time t_i and have traveled the distance between L_m and $L_m + d_m$ by time t. Hence, the total number of molecules which have left the microreactor exit and which are inside the mass spectrometer ionization cage at time t can be obtained by integration of Eq. [29],

$$C_m(t) = \int_0^t AN(t_i)\,dt_i \int_{L_m/(t-t_i)}^{(L_m+d_m)/(t-t_i)} f(U)\,dU, \qquad [30]$$

where $C_m(t)$ is the number of moles of gas molecules in the ionization cage. The function $f(U)$ is the density function of the Maxwellian velocity distribution (17), defined as

$$f(U) = 4\pi(M/2\pi RT)^{3/2}U^2 \exp\left(-\frac{MU^2}{2RT}\right), \qquad [31]$$

where M is the molecular weight, T is the temperature of the catalyst bed, and R is the universal gas constant.

The integral $\int_{L_m/(t-t_i)}^{(L_m+d_m)/(t-t_i)} f(U)\,dU$ is a function of $t - t_i$ only for given L_m and d_m. As a function of t_i, it has negligibly small values for all $t_i < t$, it rises rapidly to a sharp peak as t_i approaches t, and it falls off precipitously to zero thereafter. This integral can be approximated well by a delta function $a\delta(t_i - \bar{t})$, where the weighting factor a is $\int_0^t dt_i \int_{L_m/(t-t_i)}^{(L_m+d_m)/(t-t_i)} f(U)\,dU$, which is approximately a constant for different values of t. The time delay $\bar{t}$ is the path length between the microreactor exit and the mass spectrometer ionization cage divided by the mean molecular velocity of the gas leaving the microreactor, calculated from kinetic theory. This implies that over short distances the molecular beam with Maxwellian velocity distribution can be represented well by plug flow (i.e., by a beam with all molecules traveling at the same velocity). Moreover, since the time delay is short (e.g., 0.001 s for $L_m = 0.5$ m and a mean molecular velocity of 445 m/s for oxygen at room temperature), it can be neglected whenever the time scale of the measurement of the signal is 0.1 s or larger. Typically for TAP studies with the packed bed the time delay is two orders of magnitude less than the time scale of the response and can safely be neglected. Therefore, the response measured by the mass spectrometer $C_m(t)$ is approximately equal to the molecular flux at the microreactor exit $N(t)$ multiplied by a normalization factor K_{mb} according to the following linear relationship:

$$C_m(t) = K_{mb}N(t). \qquad [32]$$

The resulting equation [32] indicates that the concentration of gas molecules in the molecular beam of the mass spectrometer detector zone is directly proportional to the flux at the microreactor exit. The proportionality factor K_{mb} also accounts for the fact that not all of the molecules that exit the microreactor travel through the mass spectrometer detection zone (since the molecular beam from the microreactor is not collimated).

Backscattering flow. As explained above in the experimental section, the TAP reactor system used here was a precursor to the commercial version. Design features and operating characteristics of the newer commercial version TAP system are described elsewhere (2, 8). It

suffices to say that the modified geometry and reduced volume of the vacuum chamber of the commercial TAP reactor system yield higher pumping efficiencies than those obtained with the system shown by Fig. 2. In addition, a turbomolecular pump is added to the detector chamber in some commercial versions, versus an ion pump in the prototype TAP system. The features of the prototype TAP reactor system can result in molecules reentering the mass spectrometer detection zone if they are not ionized and subsequently removed from the vacuum chambers. This phenomenon can be generally considered to be molecular beam backscattering, which is clearly undesirable since it introduces a distortion of the true microreactor response, especially in the tail region. The accuracy of the transport and kinetic rate parameters can be adversely affected if backscattering is present, but not properly accounted for in the parameter estimation.

The concentration of the backscattered molecules in the vacuum chambers can be estimated by the following unsteady state mass balance:

$$V\frac{dC_b}{dt} = AN(t) - PC_b. \qquad [33a]$$

The initial condition is

$$\text{at } t = 0, \quad C_b = 0 \qquad [33b]$$

Here, the pumping rate is assumed to be first order, and the pumping speed P is assumed to be a constant. The variable C_b is the backscattering response measured by the mass spectrometer, $N(t)$ is the flux at the microreactor exit, and A is the cross-sectional area of the microreactor. Since backscattering effects can generally occur in any of the chambers shown in Fig. 2, the volume V and pumping speed P can represent some weighted average of the contributions from the individual chambers. Here, they are viewed as lumped quantities. No attempt was made here to study backscattering in detail (e.g., via Monte Carlo simulation). Therefore, V is used here as the volume of the vacuum chambers, which could mean all the chambers or one particular chamber.

The shape of the C_b versus t curve predicted by Eq. [33] depends only on the pumping frequency P/V, not on the absolute volume V, since the solution is

$$C_b(t) = \frac{A}{V}\int_0^t N(\tau)\exp\left[-\frac{P}{V}(t-\tau)\right]d\tau. \qquad [34]$$

The parameter A/V which appears in Eq. [34] can be incorporated into a single scaling parameter. Equation [34] allows the response of backscattered molecules $C_b(t)$ to be determined, provided that $N(t)$ and P/V are known.

Combined backscattering and molecular beam gas transport. The TAP response measured by the mass spectrometer primarily contains the combined responses of transport–kinetic effects that occur in the TAP microreactor, and the molecular beam and backscattering responses, assuming the latter is present. The leading edge of the response is determined mostly by the molecular beam, while the response tail can possibly contain the effects of the backscattering.

The key assumption used here is that the signal due to the molecular beam is independent of the signal caused by the backscattering. The backscattering concentration is superimposed onto the molecular beam concentration because molecules have negligible interaction in the free molecular flow regime. The final mass-spectrometer-measured signals are just superpositions of signals generated by individual molecules. The calculated mass spectrometer signal, $R(t)$, can then be expressed as a linear combination of the molecular beam contribution and the backscattering contribution according to

$$R(t) = K_b[C_b(t) + K_{mb}N(t)], \qquad [35]$$

where K_{mb}, as defined above by Eq. [32], is the parameter indicating the relative contribution of the molecular beam, and K_b is the factor that scales the calculated curve to the same height as the measured curve. The use of Eq. [35] for comparison of the TAP experimental and model predicted response is described in the next section.

Time-Domain Parameter Estimation

Application of the models for the TAP microreactor described in the previous sections to analyze experimental data is now illustrated. The models for the microreactor given by Eqs. [16] and [25] are combined with the model for free molecular flow behind the microreactor to obtain the model predicted output response. This represents the response measured by the mass spectrometer and is defined by Eq. [35]. A step-by-step procedure for determination of the model parameters by time-domain parameter estimation is described below. For simplicity, a single component system with no adsorption ($k_1 = k_2 = 0$) or reaction is considered.

1. The experimentally measured response curve is adjusted for baseline offset and each point is normalized by the area so that the area under the resulting response is unity. Let $E(t)$ be the resulting curve. The relationship between the area of the response curve and the amount of molecules introduced can be established by using an inert internal standard, such as argon or krypton, and measuring the response factor for the diffusing species relative to the internal standard. This assumes that they are pumped out at the same efficiency.

2. The molecular flux at the microreactor exit, $N(t)$, is calculated with the Knudsen diffusivity as the only adjustable parameter. Other model parameters, such as h and h_0^*, are measured directly. A parameter estimation scheme is then used to match the model-predicted and experimental responses.

3. The backscattering curve $C_b(t)$ is calculated from Eq. [34] using an assumed P/V if the model-predicted $N(t)$ curve cannot be matched with the experimental curve within a prescribed error.

4. The mass spectrometer response curve $R(t)$ is calculated using Eq. [35], where K_{mb}, P/V, and D_L are used as adjustable parameters. Then $R(t)$ curve is normalized to the same height as the normalized experimental curve.

5. By time-domain parameter fitting, the values of D_L, P/V, and K_{mb} can be determined. The values of D_L, P/V, and K_{mb} are adjusted so that the sum of the squares of errors between $R(t)$ and $E(t)$ is minimized.

RESULTS AND DISCUSSION

Backscattering Effects

An assessment of the relative contribution of backscattering was performed by interpretation of transient response measured using the TAP reactor system described above and on a newer commercial version equipped with a modified vacuum system. In both systems, an ion pump was utilized in the detector chamber. Pulsed experiments in the commercial version were performed using neon, oxygen, argon, carbon dioxide, and krypton as gases, the microreactor was packed with nonporous glass beads (d_p = 0.210 mm). Experiments in the prototype TAP reactor were performed using oxygen, carbon dioxide, $CBrF_3$, and *n*-butane with nonporous glass beads (d_p = 0.354 mm).

Figure 5 gives a comparison between the experimental and model-predicted responses obtained using the TAP system described in this work. In all cases, the contribution of backscattering is severe and had to be included to obtain good agreement between the model-predicted and experimental responses. Values for various model parameters for each gas are given in the figure legend.

Figure 6 is similar, except that the data were obtained using the new version of the TAP system. If the normalized experimental curve reflects only the molar flux at the microreactor exit resulting from Knudsen diffusion, the responses should follow the order of increasing molecular weight. However, Fig. 6 shows that the Ar (M = 40) response is lower than the CO_2 (M = 44) response and the Ne (M = 20) response is lower than the Ar, CO_2, and O_2 responses. The pattern of the curves illustrated by Fig. 6 indicates that backscattering alters the shape of the response curves even in this newer TAP system. Backscattering effects are the most severe for neon since it is

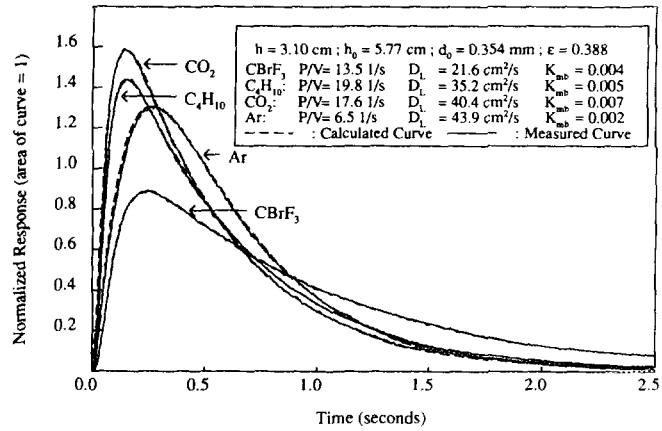

FIG. 5. Response of various gases for the prototype TAP system.

a light noble gas that is more difficult to pump than the remaining gases. Replacement of the ion pump with a turbomolecular pump should eliminate or reduce the magnitude of backscattering effects so that it might be possible to use a reduced form of the model based upon the response at the microreactor exit.

Figures 7 and 8 compare the relative contributions of molecular beam response and backscattering response to the response measured by the mass spectrometer, using carbon dioxide as the pulsed gas for the two different TAP reactor systems. The pumping frequency factor is larger in the commercial version, and the relative contribution of the molecular beam response is much larger than that obtained using the prototype TAP reactor system.

In order to provide a better view of the degree of cross-correlation between parameters and model applicability, 95% confidence intervals are tabulated in Table 1 for the parameters in Figs. 7 and 8. The relative errors of 95% confidence intervals are small, indicating that the degree of cross-correlation between parameters is small and the parameter estimation is reliable.

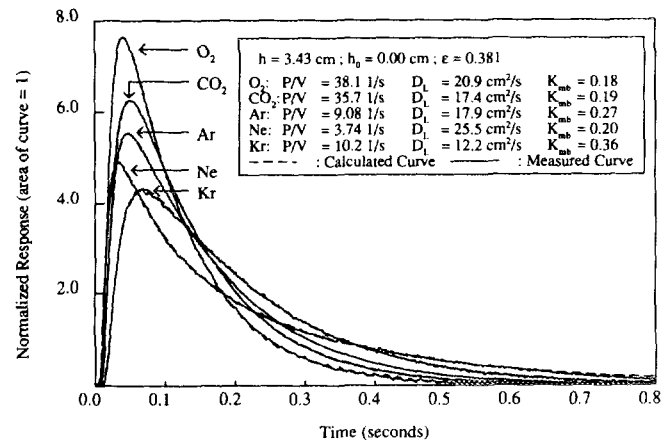

FIG. 6. Response of various gases for the commercial TAP system.

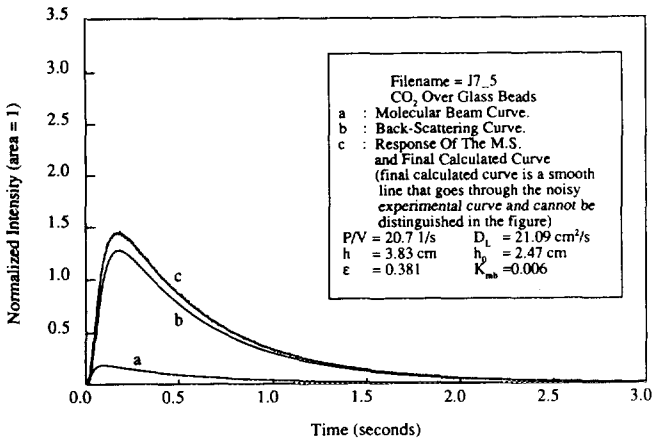

FIG. 7. Experimental and calculated response curves for the prototype TAP system.

Figure 9 shows the time-domain results for the commercial version TAP reactor system when backscattering effects are neglected. The result for oxygen is good enough for practical purposes. The result for argon is not satisfactory. The calculated Knudsen diffusivity for argon has an 18% relative error if backscattering is neglected. Since argon is often used as an inert internal standard, the error in argon diffusivity could affect the accuracy of the kinetic data. This illustrates the importance of accounting for finite pumping efficiencies when modeling the transient responses for certain gases with TAP systems having ion pumps.

Effect of Pulsed Gas Molecular Weight

As mentioned before, gases having different molecular weights were pulsed into the microreactor with the inlet section empty. The particular gases used here were CH_4, C_2H_6, Ar, CO_2, C_4H_{10}, CHF_3, and $CBrF_3$. The catalyst bed was packed with glass beads of d = 0.354 mm, the length of the catalyst bed was h = 3.10 cm, and the porosity ε was 0.388. The inlet section was empty and h_0^* = 7.19 cm. The resulting experimental curves were matched using Eq. [35]. Figure 10 shows that a linear relationship is obtained when the effective Knudsen diffusivities calculated by matching the TAP curves for various gases are plotted against $1/\sqrt{M}$, which is theoretically expected. The slope of the line is 256.5, which agrees with the value calculated from the correlation for Knudsen diffusivity developed by Huizenga and Smith (18). Similar results were reported by Gleaves *et al.* (1) and Svoboda *et al.* (8).

TABLE 1

95% Confidence Intervals for Parameters P/V, D_L, and K_{mb} in Fig. 7 and Fig. 8

	Fig. 7	Fig. 8
P/V	(20.70 ± 0.15)	(37.41 ± 0.99)
$\Delta(P/V)/(P/V)$	7.2×10^{-3}	0.026
D_L	(21.09 ± 0.03)	(17.34 ± 0.04)
$\Delta D_L/D_L$	1.4×10^{-3}	2.3×10^{-3}
K_{mb}	$(0.006 \pm 0.26 \times 10^{-3})$	(0.1833 ± 0.009)
$\Delta K_{mb}/K_{mb}$	0.043	0.049

Effect of the Inlet Section Length

Equation [17] shows that the first absolute moment has a linear dependence on the length of the inlet section. To provide experimental verification of this result, oxygen was pulsed into a bed of glass beads. The parameter $L = h_0^*/(h\varepsilon)$ was varied by changing h_0^*, which is the equivalent length of the empty section in front of the catalyst bed. The remaining experimental conditions were held constant. Figure 11 shows the results of changing the length of the inlet section, which confirms the validity of the first absolute moment since the correlation coeffi-

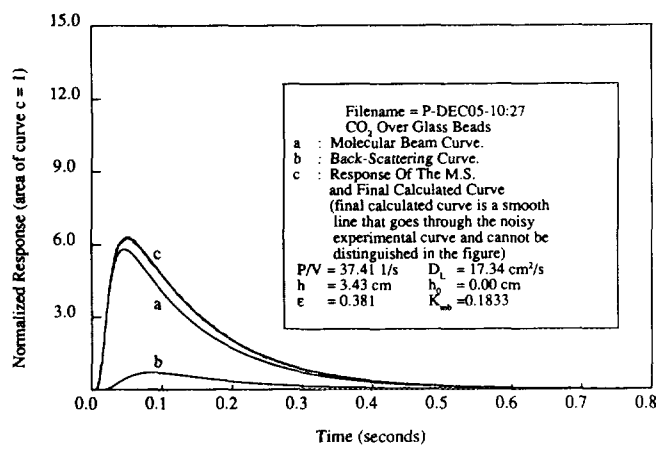

FIG. 8. Experimental and calculated response curves for the commercial TAP system.

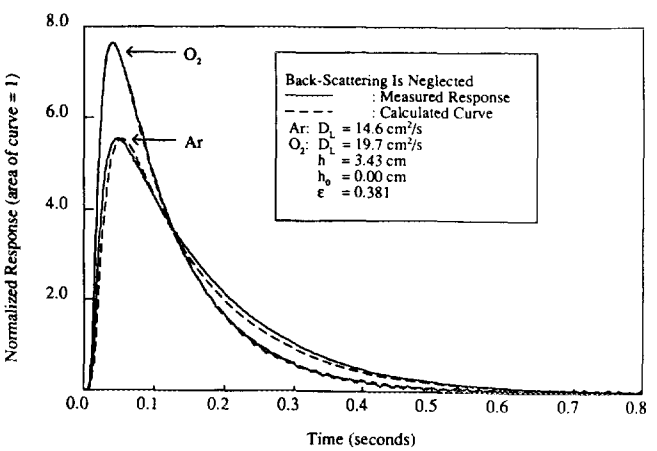

FIG. 9. Time-domain matching of the response curves for the commercial TAP system without considering backscattering.

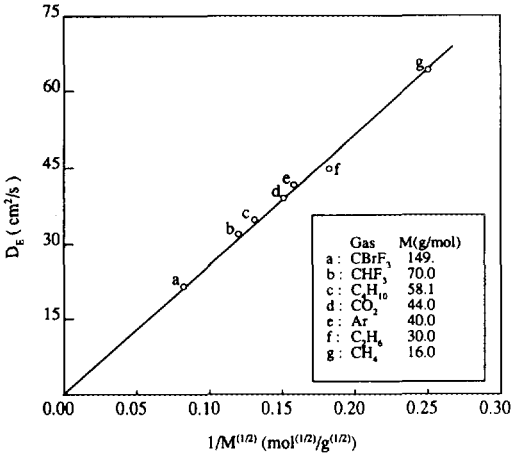

FIG. 10. Diffusivity changes with molecular weight.

cient for this line is 0.9972. Equation [17] indicates that the adsorption equilibrium constant calculated from this expression will be larger than the true value if the effect of L is not properly accounted for.

Determination of Heats of Adsorption

To illustrate one application of the model, the determination of the heat of adsorption for acrolein on Bi_2MoO_6 is considered by analysis of TAP reactor transient response data (1).

The first absolute moment given by Eq. [17] can be expressed in the following forms, where the subscripts a and i correspond to the adsorbing and nonadsorbing or inert gas, respectively:

$$t_{1a} = \frac{h^2\varepsilon}{2D_L}\left(1 + 2\frac{h_0^*}{h\varepsilon} + \rho_p\frac{(1-\varepsilon)}{\varepsilon}\frac{k_1}{k_2}\right) \quad [36]$$

$$t_{1i} = \frac{h^2\varepsilon}{2D_L}\left(1 + 2\frac{h_0^*}{h\varepsilon}\right). \quad [37]$$

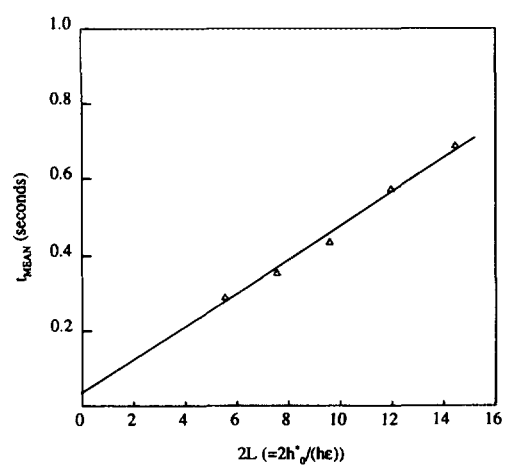

FIG. 11. First moment changes with L ($= h_0^*/(h\varepsilon)$).

If the rate constants are expressed in the Arrhenius form, the above equations can eventually be expressed as

$$\ln\left(t_{1a} - t_{1i}\sqrt{\frac{M_a}{M_i}}\right)\sqrt{T} = C + \frac{E_d - E_a}{RT}. \quad [38]$$

This relationship shows that a plot of $\ln(t_{1a} - t_{1i}\sqrt{M_a/M_i})\sqrt{T}$ versus $1/T$ should yield a straight line with a slope equal to $(E_d - E_a)/R$.

The data given in Fig. 14 in the paper of Gleaves *et al.* (1) were reanalyzed using Eq. [38], plotted in Fig. 12. This yields E_d = 22.2 kcal/mol, which is 5.2 kcal/mol greater than the value reported by Gleaves *et al.* (1). The reason for this difference is that the equation presented by Gleaves *et al.* (1) does not account for the effect of temperature on the diffusivity of the inert gas. Matsuura (19) measured the heat of adsorption in the same chemical system by monitoring pressure changes in a system of constant volume. A value of E_d = 21.2 kcal/mol was obtained by his method. Our result based on the TAP experiments of Gleaves *et al.* (1) is within 5% of Matsuura's value.

Uniqueness of Kinetic Parameters and Kinetic Models

A legitimate question can be raised regarding the uniqueness of kinetic models and the associated kinetic and adsorption/desorption parameters when data from the TAP reactor are used as the basis for the determination of these parameters from a single pulse response curve or other type of TAP reactor response.

A detailed analysis of model discrimination and parameter estimation using TAP reactor data is complicated enough to be the subject of a separate study and lies outside the scope of this work. However, we have partially addressed this question by analyzing the ability of a single-site adsorption model to match the single pulse TAP response curve obtained by simulating dual-site adsorption phenomena when the sites had different adsorp-

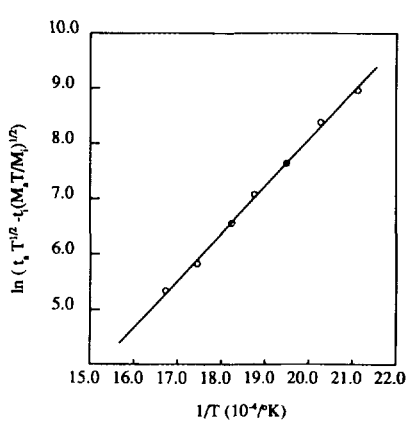

FIG. 12. Activation energy plot for acrolein desorption.

tion constants and desorption activation energies. Most often, at a single temperature, the TAP response obtained from the single-site model was able to fit the dual-site response with little or no significant error. However, if single pulse TAP responses were generated at a series of temperatures, the dual-site model achieves a better fit of all the data than the single-site model. Whether the differences in fits obtained are significant to allow statistically valid model discrimination was not examined in detail and remains a topic for future work.

Our brief analysis of this issue reveals that interpretation of TAP reactor data is prone to the same pitfall as interpretations of other transient response experiments, namely, that uniqueness of the model and associated parameters obtained by parameter estimation methods cannot be guaranteed if two or more parameters were used in the model. This, however, does not diminish the usefulness of obtaining a quantitative fit for a particular model. Based on the understanding of the chemistry for each particular case studied, possible alternative models can be formulated. A combination of various experimental techniques can then be used to independently evaluate some parameters in these models. A properly designed series of TAP experiments under different conditions, such as reactor temperature and pulse concentration, can then address the quantification of the remaining parameters. If discrimination of alternative models is still not achieved with statistical significance, additional TAP and/or other experiments must be designed.

SUMMARY AND CONCLUSIONS

Models of the TAP system which include the fast pulsing valve, the microreactor, and the free molecular flow behind the microvector were developed in this work. It was shown that the Knudsen diffusion equation can be used to describe the motion of the gas in the TAP microreactor. The use of zero concentration as the boundary condition at the microreactor exit was justified theoretically and shown to lead to correct results. Using the Knudsen diffusion model, transport of the gas in a TAP microreactor packed with nonporous and porous catalyst particles can be successfully described. The models developed here are more general than previous models. The effect of the particular method used to pack the microreactor entrance zone and the effect of the catalyst pore structure on the measured TAP transient responses can be interpreted using these models.

It was shown that both molecular beam and backscattering flows contribute to the signal measured by the mass spectrometer. Equipment design and vacuum pump type and capacity, as well as the microreactor positioning, affect the amount of backscattering. Backscattering is minimized by positioning the microreactor closer to the mass spectrometer. It was demonstrated that the mass spectrometer signal can be treated as a linear combination of molecular beam and backscattering contributions.

Time-domain matching of TAP responses leads to accurate estimates of diffusivities of various gases in packed beds. Good estimates of activation energy for adsorption can also be obtained. The model presented also illustrates the considerable effect that the microreactor entrance zone can have on the measured response. The modeling and solution methodology presented here can be extended readily to describe more complex linear phenomena in the TAP system.

It was also found that adsorption–desorption parameters evaluated from a single pulse TAP response curve may not be unique. However, the physical transport model presented here makes possible the investigation of various forms of adsorption–desorption models in terms of their ability to match the observed response. This should aid in preparing a viable experimental strategy for model discrimination.

APPENDIX: NOMENCLATURE

A	cross-sectional area of the microreactor, cm^2
C	gas-phase concentration in the catalyst bed, mol/cm^3
C_b	concentration inside mass spectrometer detector contributed by backscattering flow, mol/cm^3
C_p	gas-phase concentration in the catalyst particle, mol/g
C_{ads}	solid-phase concentration in the catalyst bed, mol/g
C^*	equivalent gas-phase concentration in the inlet section, mol/cm^3
C_0^*	equivalent initial gas-phase concentration in the inlet section, mol/cm^3
C_m	number of moles of gas inside mass spectrometer detector contributed by molecular beam transport, mol
$\bar{C}$	gas-phase concentration in the Laplace domain, $mol \cdot s/cm^3$
D	duration setting of the fast pulsing valve
D_L	effective Knudsen diffusivity in the catalyst bed, cm^2/s
D_S	effective Knudsen diffusivity inside the particle, cm^2/s
D_t	duration of the fast pulsing valve, μs
d_m	effective length of the mass spectrometer detector, m
$f(U)$	velocity distribution density function
f	frequency, 1/s
h	length of the catalyst bed, cm
h_0	length of the inlet section in front of the catalyst bed, cm

h_0^* equivalent length of the inlet section in front of the catalyst bed which only accounts for the empty space, cm
I intensity setting of the fast pulsing valve
I_{t0} opening time constant of the fast pulsing valve, μs
I_t opening time of the fast pulsing valve, μs
K_a physical adsorption equilibrium constants, g/cm^3
k_1 physical adsorption rate constants, cm^3/(g · s)
k_2 physical desorption rate constants, 1/s
k_{ads} physical adsorption rate constants, cm^3/(g · s)
K_{mb} a number indicating relative importance of the molecular beam
K_b scaling factor
L_m length from the microreactor outlet to the mass spectrometer, m
M molecular weight, kg/mol
$N(t)$ molecular flux at the microreactor exit, mol/cm^2 s
N_t total number of molecules pulsed
$\bar{N}(s)$ flux at the microreactor exit in the Laplace domain, mol/cm^2
P pumping speed of the vacuum system, m^3/s
P_0 feed pressure, atm
R the universal gas constant, 8.314 J/(mol · K)
R catalyst particle radius, cm
r radial direction, cm
$R(t)$ the mass spectrometer measured response curve
s independent variable in the Laplace domain, 1/s
T temperature, K
T_0 feed temperature, K
t_{1a} mean residence time of reactive gas, s
t_{1i} mean residence time of inert gas, s
t time, s
$\bar{t}$ gas mean residence time or the first moment of $N(t)$, s
U molecular velocity of gas molecules, m/s
v mean molecular velocity of gas molecules at the exit of the microreactor, m/s
V volume of the vacuum chambers, m^3
x x coordinate, cm

Greek Letters

β $KLVN_{av} = 3.52 \times 10^{14}$
β porosity of the particles
γ the ratio of specific heats, C_p/C_v
ε_1 dimensionless number = $D_L/(vh)$
ε porosity of the catalyst bed
η dimensionless length = x/h
ϕ working variable, defined by Eq. [15], cm^{-1}
Ψ working variable, defined by Eq. [26], cm^{-1}
ψ working variable, defined by Eq. [27], cm^{-1}
ρ_p density of the catalyst particle, g/cm^3
σ^2 variance of the response curve, s^2

ACKNOWLEDGMENTS

This study was sponsored by the industrial participants of the Chemical Reaction Engineering Laboratory at Washington University and the K. C. Wong Education Foundation.

REFERENCES

1. Gleaves, J. T., Ebner, J. R., and Kuechler, T. C., *Catal. Rev. Sci. Eng.* **30**(1), 49 (1988).
2. Gleaves, J. T., Ebner, J. R., and Mills, P. L., *in* "Catalysis 1987, Proceedings 10th North American Meeting of the Catalysis Society" (J. W. Ward, Ed), Vol. 38, p. 633. Elsevier, Amsterdam, 1988.
3. Bird, G. A., "Molecular Gas Dynamics." Clarendon, Oxford, 1976.
4. Lei, D., Chen, S., Gleaves, J. T., and Gaspar, P. P., *in* "25th Silicon Symposium, Los Angeles, CA, April 3–4, 1993."
5. Pepera, M. A., Callahan, J. L., Desmond, M. J., Milberger, E. C., Blum, P. R., and Bremer, N. J., *J. Am. Chem. Soc.* **107,** 4883 (1985).
6. Centi, G., Fornasari, G., and Trifiro, F. *J. Catal.* **89,** 44 (1984).
7. Morselli, L., Trifiro, F., and Urban, L., *J. Catal.* **75,** 112 (1982).
8. Svoboda, G. D., Gleaves, J. T., and Mills, P. L., *Ind. Eng. Chem. Res.* **Jan.,** 19 (1992).
9. Zou, B. S., "Modeling the System for Temporal Analysis of Products (TAP)." Doctoral Dissertation, Washington University, St. Louis, MO 63130, May, 1992.
10. Froment, G. F., and Hoosten, L. H., *in* "Catalysis—Science and Technology" (J. R. Anderson and M. Boudart, Eds.), Vol. 1, p. 98. Springer-Verlag, Berlin, 1981.
11. Mills, P. L., and Duduković, M. P., *AIChE J.* **34,** 1752 (1988).
12. Rigas, N. C., Svoboda, G. D. and Gleaves, J. T., *in* "Catalytic Selective Oxidation" (J. U. Hightower and S. T. Oyama, Eds.), ACS Symposium Series, Vol. 523, 183. Am. Chem. Soc., Washington, DC, 1993.
13. Duduković, M. P., *in* "Chemical Reactor Design and Technology (H. I. Delasa, Ed.) NATO ASI Series E, No. 110, p. 107. Martinus Nijhoff, Dordrecht, 1986.
14. Hirschfelder, J. G., Curtiss, C. F., and Bird, R. B., "Molecular Theory of Gases and Liquids." Wiley, New York, 1964.
15. Furusawa, T., Suzuki, M., and Smith, J. M., *Catal. Rev. Sci. Eng.* **13**(1), 43 (1976).
16. Cooley, J. W., Lewis, P. A. W., and Welch, P. D., *J. Sound Vibration* **12**(3), 315 (1970).
17. Liepmann, H. W., and Roshko, A., "Elements of Gas Dynamics." Wiley, New York, 1957.
18. Huizenga, D. G., and Smith, D. M., *AIChE J.* **32**(1) (Jan. 1986).
19. Matsuura, I., *J. Catal.* **33,** 420 (1974).